

RESEARCH ARTICLE

Curcumin suppresses cell proliferation and triggers apoptosis in vemurafenib-resistant melanoma cells by downregulating the EGFR signaling pathway

Yu-Jen Chiu^{1,2,3} | Jai-Sing Yang⁴  | Fuu-Jen Tsai^{5,6,7} | Hong-Yi Chiu^{8,9,10} | Yu-Ning Juan⁴ | Yu-Hsiang Lo⁴ | Jo-Hua Chiang¹¹ 

¹Division of Plastic and Reconstructive Surgery, Department of Surgery, Taipei Veterans General Hospital, Taipei, Taiwan

²Department of Surgery, School of Medicine, National Yang Ming Chiao Tung University, Taipei, Taiwan

³Institute of Clinical Medicine, National Yang Ming Chiao Tung University, Taipei, Taiwan

⁴Department of Medical Research, China Medical University Hospital, China Medical University, Taichung, Taiwan

⁵Human Genetic Center, China Medical University Hospital, Taichung, Taiwan

⁶Department of Medical Genetics, China Medical University Hospital, Taichung, Taiwan

⁷School of Chinese Medicine, China Medical University, Taichung, Taiwan

⁸Department of Pharmacy, Hualien Tzu Chi Hospital, Buddhist Tzu Chi Medical Foundation, Hualien, Taiwan

⁹Graduate Institute of Clinical Pharmacy, College of Medicine, Tzu Chi University, Hualien, Taiwan

¹⁰Holistic Education Center, Tzu Chi University of Science and Technology, Hualien, Taiwan

¹¹Department of Nursing, Chung-Jen Junior College of Nursing, Health Sciences and Management, Chiayi, Taiwan

Correspondence

Jo-Hua Chiang, Department of Nursing, Chung-Jen Junior College of Nursing, Health Sciences and Management, No. 1-10 Da-Hu, Hubei Village, Dalin Township, Chiayi County 622001, Taiwan.
Email: j588011430@gmail.com

Funding information

Chung-Jen Junior College of Nursing, Health Sciences and Management, Grant/Award Numbers: 108-011 and 109-010; China Medical University Hospital, Grant/Award Number: DMR-110-136; Melissa Lee Cancer Foundation, Grant/Award Number: MLCF-V110-11001; Taipei Veterans General Hospital, Grant/Award Number: V110B-038; Yen Tjing Ling Medical Foundation, Grant/Award Number: CI-110-6

Abstract

Melanoma is a malignant tumor with aggressive behavior. Vemurafenib, a BRAF inhibitor, is clinically used in melanoma, but resistance to melanoma cytotoxic therapies is associated with *BRAF* mutations. Curcumin can effectively inhibit numerous types of cancers. However, there are no reports regarding the correlation between curcumin and vemurafenib-resistant melanoma cells. In this study, vemurafenib-resistant A375.S2 (A375.S2/VR) cells were established, and the functional mechanism of the epidermal growth factor receptor (EGFR), serine–threonine kinase (AKT), and the extracellular signal-regulated kinase (ERK) signaling induced by curcumin was investigated in A375.S2/VR cells *in vitro*. Our results indicated that A375.S2/VR cells had a higher IC₅₀ concentration of vemurafenib than the parental A375.S2 cells. Moreover, curcumin reduced the viability and confluence of A375.S2/VR cells. Curcumin triggered apoptosis via reactive oxygen species (ROS) production, disruption of mitochondrial membrane potential ($\Delta\Psi_m$), and intrinsic signaling (caspase-9/-3-dependent) pathways in A375.S2/VR cells. Curcumin-induced apoptosis was also mediated by the EGFR signaling pathway. Combination treatment with curcumin and gefitinib (an EGFR inhibitor) synergistically potentiated the inhibitory effect of cell viability in A375.S2/VR cells. The present study provides new insights into the

Yu-Jen Chiu and Jai-Sing Yang contributed equally to this study.

therapy of vemurafenib-resistant melanoma and suggests that curcumin might be an encouraging therapeutic candidate for its drug-resistant treatment.

KEYWORDS

apoptosis, EGFR, melanoma, vemurafenib, vemurafenib-resistant A375.S2 cells

1 | INTRODUCTION

Cutaneous melanoma is a malignant tumor with aggressive behavior. Although the incidence is comparatively low in the Asian population, it has been increasing in recent years.¹ There are four main histological subtypes of cutaneous melanoma: superficial spreading melanoma, nodular melanoma, lentigo malignant melanoma, and acral lentiginous melanoma.² Ultraviolet and skin pigmentation are thought to play major roles in the development of cutaneous melanoma.^{2,3}

Surgical wide excision of the tumor, including the surrounding tissue, is the primary treatment strategy for early stage and localized melanoma.⁴ Furthermore, sentinel lymph node biopsy should be performed in patients whose tumor is ulcerated or the depth of the tumor is greater than 0.8 mm.^{4,5} As cancer cells invade lymph nodes, their prognosis is dramatically reduced.⁶ The response rate to traditional chemotherapy is very poor.^{6,7} Recently, the response rates and overall survival in patients with BRAF-mutant advanced melanoma have been greatly improved by BRAF inhibitors, including vemurafenib, dabrafenib, and encorafenib.⁸ However, serious adverse effects, including cutaneous squamous cell carcinoma, left ventricular dysfunction, and ocular events, have attenuated this kind of therapy. Furthermore, drug resistance is easily developed, especially in Asian population.^{8,9} There is an unmet need for effective therapy in patients with progressive melanoma, especially those resistant to BRAF inhibitors.

Chemical compounds or substances derived from natural products have become a significant source of therapeutic candidates for cancer patients.¹⁰ Curcumin has been broadly used in traditional Chinese medicine for centuries in Asia and is derived from *Curcuma longa* plant.¹¹ Curcumin has been reported to have several pharmacological functions, including anti-inflammatory, antibacterial, antidepressant, antioxidant, antidiabetic, antiviral, and anticancer properties.^{11–13} Curcumin has been reported to effectively inhibit numerous types of cancer cell growth through various signaling pathways, including inducing autophagy, apoptosis, and cell cycle arrest.¹⁴ Currently, curcumin has been shown in clinical trials in patients with pancreatic cancer, multiple myeloma, colon cancer, and head and neck cancer.^{11,14}

To date, several studies have reported that curcumin inhibits the growth of human melanoma.^{12,13,15–17} However, to the best of our knowledge, there are no reports regarding the correlation between curcumin and vemurafenib-resistant melanoma cells. The present study is to investigate curcumin-triggered cell growth inhibition and apoptotic death in human malignant melanoma vemurafenib-resistant A375.S2 cells (A375.S2/VR) *in vitro*. Based on our results, the induction of apoptotic death in A375.S2/VR cells caused by curcumin was

mediated through epidermal growth factor receptor (EGFR)-mediated and mitochondria-dependent signaling pathways.

2 | MATERIAL AND METHODS

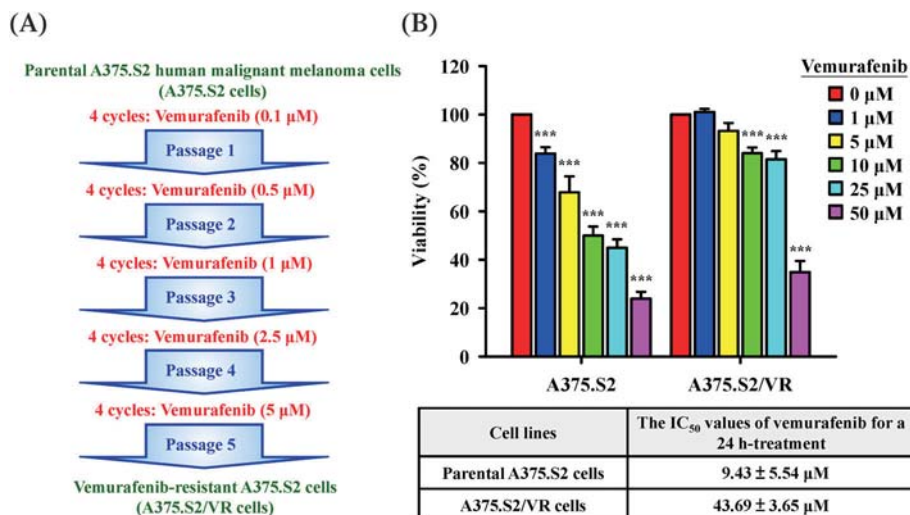
2.1 | Chemicals and reagents

Curcumin, 4',6-diamidino-2-phenylindole (DAPI), dimethyl sulfoxide (DMSO), propidium iodide (PI), vemurafenib (VPC-13566), thiazolyl blue tetrazolium bromide (MTT), gefitinib, Z-VAD-FMK, Z-DEVD-FMK, Z-LEHD-FMK, and *in situ* cell death detection kit, fluorescein were purchased from Merck KGaA (Darmstadt, Germany). CellTracker Green CMFDA Dye, CM-H₂DCFDA, fetal bovine serum (FBS), JC-1, L-glutamine, minimum essential medium (MEM), penicillin, streptomycin, and trypsin-EDTA were obtained from Thermo Fisher Scientific (Waltham, MA, USA). The Annexin V-FITC Apoptosis Detection Kit was purchased from Strong Biotech Corporation (Taipei, Taiwan). FAM-fluorochrome-labeled inhibitor of caspases assay (FLICA) Caspases-3/7 Assay Kit and FAM-FLICA Caspase-9 Assay Kit were purchased from ImmunoChemistry Technologies, LLC (Bloomington, MN, USA). All primary antibodies and goat anti-rabbit or anti-mouse immunoglobulin G secondary antibodies conjugated with horseradish peroxidase (HRP) were purchased from GeneTex International Corporation (Hsinchu, Taiwan).

2.2 | Cell line and cell culture

The human malignant melanoma A375.S2 cell line was obtained from the Bioresource Collection and Research Center, Food Industry Research and Development Institute (Hsinchu, Taiwan). Cells were cultured in 75-cm² tissue culture flasks in MEM supplemented with 2 mM L-glutamine, 10% FBS, 100 U/ml penicillin, and 100 µg/ml streptomycin at 37°C with 5% CO₂.¹⁸ Vemurafenib-resistant A375.S2 cells were established according to the protocol shown in Figure 1A. Parental A375.S2 cells were exposed to an initial concentration of vemurafenib (0.1 µM), and surviving cells were cultured to 90% confluence for four passages (3 weeks). Surviving cells were exposed to vemurafenib (0.5 µM) for four passages (3 weeks) before further 1, 2.5, and 5 µM vemurafenib treatment for four passages (3 weeks). Finally, surviving cells were exposed to 5 µM vemurafenib, as previously described.¹⁹ Surviving resistant vemurafenib-resistant A375.S2 cells were named A375.S2/VR cells, which were cultured in MEM (2 mM L-glutamine, 10% FBS, 100 U/ml penicillin, and 100 µg/ml

FIGURE 1 Establishment of vemurafenib-resistant A375.S2 cells (A375.S2/VR cells) and comparison of cell viability between parental A375.S2 human melanoma cells and A375.S2/VR cells. (A) Flowchart of A375.S2/VR cell establishment after vemurafenib treatment. (B) The cells were incubated with vemurafenib (0, 1, 5, 10, 25, and 50 μM) for 24 h. The viability of both cells was detected by an thiazolyl blue tetrazolium bromide (MTT) assay. Each point represents the mean \pm SD of three experiments; *** $p < .001$ versus control



streptomycin) plus 5 μM vemurafenib for the subsequent all experiments.

2.3 | Cell viability assay

Parental A375.S2 cells or A375.S2/VR cells (1×10^4 cells/well) were seeded into 96-well plates and treated with or without curcumin (1, 5, 10, 25, and 50 μM) or in the presence or absence of 10 μM Z-VAD-FMK (a pan-caspase inhibitor), 10 μM Z-DEVD-FMK (a caspase-3 inhibitor), 10 μM Z-LEHD-FMK (a caspase-9 inhibitor) or 20 μM gefitinib (an EGFR tyrosine kinase inhibitor) incubation, respectively, at 37°C for 24 h with 5% CO_2 . Cell viability was assessed using the MTT assay, as previously described.^{20–22}

2.4 | Cell confluence assay

A375.S2/VR cells (1×10^4 cells/well) into a 96-well plate were incubated with or without 12.5 μM curcumin for 24 h at 37°C. Cells were visualized and photographed via the IncuCyte S3 ZOOM System instrument (High-Throughput Imaging System Analysis, Essen BioScience, MI, USA) to conduct the cell confluence assay, as previously described.²³

2.5 | Three-dimensional (3D)-spheroid cell death assay

A375.S2/VR cells (5×10^3 cells/total) were stained with 10 μM CellTracker Green CMFDA Dye and seeded into 96-well Tantt SpherTantrix plates (GHP140696-10, Tantt, Taoyuan, Taiwan) for 3 days following the manufacturer's instructions.^{24,25} A375.S2/VR cells were treated with 1 $\mu\text{g}/\text{ml}$ PI and then treated with or without 12.5 μM curcumin for 24 h and 48 h at 37°C. The IncuCyte S3 ZOOM System instrument (High-Throughput Imaging System Analysis) was

used to conduct the PI staining of the cell death assay, as previously described.²⁶

2.6 | Annexin V/PI/DAPI apoptosis assay

A375.S2/VR cells (1×10^4 cells/well) were treated with or without 12.5 μM curcumin for 1, 2, 3, 4, 5, 6, 9, and 12 h. The cells were then stained with Annexin V-FITC/PI (Annexin V-FITC Apoptosis Detection Kit) and 1 $\mu\text{g}/\text{ml}$ DAPI before being seeded into 96-well plates (CellCarrier-96, TC, Black and Optically Clear Bottom, PerkinElmer, Waltham, MA, USA). High-content imaging system analysis (Molecular Devices ImageXpress Micro Confocal, San Jose, CA, USA) was used to conduct the Annexin V/PI/DAPI apoptosis assay, as previously described.²⁷

2.7 | Cell cycle and apoptosis analysis

A375.S2/VR cells were seeded (1×10^5 cells/well) into 48-well plates and treated with or without 12.5 μM curcumin for 6, 12, and 24 h at 37°C with 5% CO_2 . Cells were collected and thoroughly resuspended in 250 μl Solution 10 (lysis buffer) supplemented with PI (10 $\mu\text{g}/\text{ml}$). Cells were then incubated at 37°C for 5 min, and 250 μl Solution 11 (stabilization buffer) was added to proceed further step. After that, the cells were analyzed to engage the NucleoCounter NC-3000 Advanced Image Cytometer (ChemoMetec A/S, Allerod, Denmark) using NucleoView NC-3000 software (version 1.4) (ChemoMetec A/S). Cellular fluorescence was quantified and DNA content histograms in different cell cycle stages were displayed, as previously described.^{23,27}

2.8 | Terminal deoxynucleotidyl transferase dUTP nick end labeling (TUNEL) staining

A375.S2/VR cells (1×10^6 cells/well) into 6-well plates were exposed to 12.5 μM curcumin for 24 h at 37°C with 5% CO_2 . An in situ cell

death detection kit, fluorescein was used according to the manufacturer's protocol. TUNEL-positive cells were analyzed using a NucleoCounter NC-3000 imaging cytometer using the built-in TUNEL assay program. The cell suspension (30 μ l cell suspension) was immediately loaded into a 2-chamber slide (NC-Slide A2) (ChemoMetec A/S) for analysis according to the manufacturer's protocol. All samples were analyzed using NucleoView NC-3000 software (version 1.4), as previously described.^{26,28}

2.9 | Intracellular reactive oxygen species (ROS) and mitochondrial membrane potential ($\Delta\Psi_m$) assays by imaging cytometry

A375.S2/VR cells were seeded (1×10^6 cells/well) into 6-well plates and treated with or without 12.5 μ M curcumin for 12 h at 37°C with 5% CO₂. Cells were individually incubated with 5 μ M CM-H₂DCFDA (a general oxidative stress indicator) and 10 μ g/ml JC-1 (a mitochondrial membrane potential probe) for 30 min and then trypsinized. The 30 μ l cell suspension was immediately loaded into a 2-chamber slide (NC-Slide A2) for analysis using the NucleoCounter NC-3000 Advanced Image Cytometer according to the manufacturer's protocol. All samples were analyzed using NucleoView NC-3000 software (version 1.4), as previously described.^{27,29,30}

2.10 | Caspase-9 and caspase-3 activities assay

A375.S2/VR cells (1×10^6 cells/well) into 6-well plates were treated with or without 12.5 μ M curcumin for 6, 12, and 24 h at 37°C. The cells were harvested and re-suspended with diluted the FLICA reagent and Hoechst 33342, according to the manufacturer's protocol (FAM-FLICA Caspases-3/7 Assay Kit and FAM-FLICA Caspase-9 Assay Kit) for 1 h at 37°C. After washing, cells were resuspended in 100 μ l apoptosis wash buffer supplemented with PI. The 30 μ l cell suspension was immediately loaded into a 2-chamber slide (NC-Slide A2) for analysis on the NucleoCounter NC-3000 Advanced Image Cytometer using the built-in caspase assay program, as previously described.^{26,27}

2.11 | Western blot

A375.S2/VR cells were seeded (1×10^7 cells/total) into 75-T flasks and treated with or without 12.5 μ M curcumin for 12 h at 37°C with 5% CO₂. Whole cell lysates were prepared and lysed in Trident RIPA Lysis Buffer (GeneTex). The protein content of the supernatant was measured using a Bio-Rad Protein Assay Kit (Bio-Rad, Hercules, CA, USA), and approximately 40 μ g of total protein lysate was separated on 10% sodium dodecyl sulfate (SDS)-polyacrylamide gel electrophoresis (PAGE) gels for 1 h and subsequently electrotransferred onto an

Immobilon-P Transfer Membrane (Merck Millipore), as described previously.^{28,31} Membranes were blocked with 5% non-fat dry milk in 1 \times TBS-T (20 mM Tris-HCl, pH 7.6, 137 mM NaCl, and 0.1% Tween-20) for 1 h at room temperature and immunoblotted with the primary antibodies against EGFR (phospho Tyr1068) (cat. No. GTX00975), EGFR (cat. No. GTX628888), AKT (phospho Ser473) (cat. No. GTX50128), AKT (cat. No. GTX128415), ERK1 (phospho Tyr204)/ERK2 (phospho Tyr187) (cat. No. GTX50275), ERK1/2 (cat. No. GTX134462) at a dilution of 1:500, and β -Actin (cat. No. GTX109638) at a dilution of 1:3000 at 4°C overnight. The blots were then probed with appropriate HRP-conjugated secondary antibodies for 1 h at room temperature and developed using chemiluminescence using Immobilon Western Chemiluminescent HRP Substrate (Merck Millipore), as described previously.³¹⁻³³ Quantitative analysis of each blot was performed to quantify the intensity of the band signal using the National Institutes of Health (NIH) ImageJ program version 1.8.0_172.

2.12 | Statistical analysis

Data are expressed as mean \pm standard deviation (SD). Statistical analyses were performed using one-way analysis of variance (ANOVA) followed by Dunnett's post hoc test using SPSS software (version 16.0) (SPSS, Chicago, IL, USA). Statistically significant differences among the means were set at *** $p < .001$ or ### $p < .001$.

3 | RESULTS

3.1 | Effects of viability on A375.S2 melanoma parental cells and A375.S2/VR cells with vemurafenib treatment

A drug-resistant cell line was established by modifying the conditions of cancer patients by chemotherapy (Figure 1A), and drug-resistant cell lines displayed between two- and eight-fold resistance compared to their parental cell line. The anti-proliferative effects of vemurafenib on A375.S2 melanoma parental cells and vemurafenib-resistant A375.S2 melanoma cells (A375.S2/VR) were detected by the MTT assay. The results demonstrated that cell viability was significantly inhibited by vemurafenib at 1–50 μ M in a concentration-dependent manner (Figure 1B, top panel). However, vemurafenib at 1–5 μ M had insignificant effects on newly established A375.S2/VR cells. The results revealed that the newly established A375.S2/VR cells had a decreased sensitivity to vemurafenib compared to the A375.S2 parental cells. We further determined the half-maximal inhibitory concentration (IC₅₀) values of vemurafenib in A375.S2 melanoma parental cells and A375.S2/VR cells. The A375.S2 parental cells were with a low IC₅₀ value (9.43 ± 5.54 μ M), but A375.S2/VR cells were with a higher IC₅₀ value (43.69 ± 3.65 μ M) (Figure 1B, bottom panel). Our results suggest that the sensitivity of A375.S2/VR cells to vemurafenib is

markedly reduced following long-term vemurafenib treatment with gradually increasing concentrations.

3.2 | Effects of curcumin on viability or confluence of A375.S2 parental cells and A375.S2/VR cells

Both of the cells were treated with curcumin (6.25, 12.5, 25, and 50 μM) for 24 h. The MTT assay showed that curcumin significantly decreased cell viability in A375.S2 parental cells (Figure 2A) and A375.S2/VR cells (Figure 2B) in a concentration-dependent manner. The IC_{50} values for curcumin in A375.S2 parental cells and A375.S2/VR cells were approximately $13.57 \pm 3.27 \mu\text{M}$ and $12.29 \pm 2.06 \mu\text{M}$, respectively. Real-time image analysis of A375.S2/VR cells using the IncuCyte S3 Kinetic Live Cell Imaging System demonstrated that curcumin obviously reduced cell confluence in a time-dependent manner (Figure 3). A dynamic time-point video also can be seen in Video S1.

3.3 | Effects of curcumin on 3D-spheroid cell death in A375.S2/VR cells

A375.S2/VR 3D-spheroid cells were treated with or without 12.5 μM curcumin for 24 h and 48 h. PI staining assay and IncuCyte S3 Kinetic Live Cell Imaging System showed that curcumin significantly induced cell death after 24 h and 48 h of treatments (Figure 4). Our data revealed that curcumin showed cytotoxicity against A375.S2/VR cells via a 3D-spheroid model.

3.4 | Effects of curcumin on early stage of apoptotic cell death in A375.S2/VR cells

To detect early apoptotic death in A375.S2/VR cells by curcumin, cell apoptosis was assessed by performing Annexin V/PI/DAPI triple staining through confocal imaging in 12.5 μM curcumin-treated A375.S2/VR cells. Confocal image analysis results demonstrated that the number of early stage apoptotic cells (Annexin V⁺/PI⁻) (green fluorescence) increased from 1 h to 6 h in curcumin-treated cells (Figure 5). In addition, the number of late stage apoptotic cells (Annexin V⁺/PI⁺) (red fluorescence) were increased in 9 h and 12 h curcumin-treated

cells (Figure 5). Our results further indicated that A375.S2/VR cell apoptosis was induced by curcumin treatment.

3.5 | Effects of curcumin on cell cycle progression and apoptosis in A375.S2/VR cells

To confirm whether curcumin affects cell cycle progression and apoptosis, A375.S2/VR cells were administered with or without 12.5 μM curcumin for 6, 12, and 24 h. The percentage of cells in sub-G1 (apoptosis), G0/G1, S, and G2/M phases was analyzed by NucleoCounter NC-3000 imaging cytometry using the 2-step cell cycle assay program (Figure 6A). Our data showed that curcumin increased the cell population in the sub-G1 phase and decreased the G0/G1, S, and G2/M phases in A375.S2/VR cells (Figure 6B).

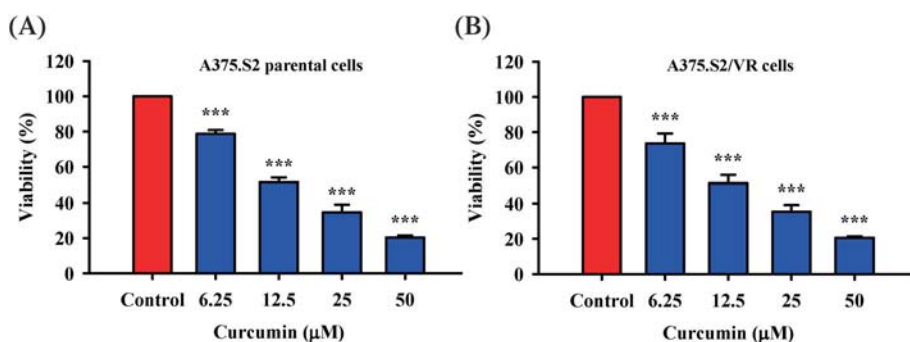
3.6 | Effects of curcumin on DNA fragmentation, ROS production, and mitochondrial membrane potential ($\Delta\Psi\text{m}$) levels in A375.S2/VR cells

We examined DNA fragmentation in curcumin-treated A375.S2/VR cells. Our results from TUNEL staining showed that 12.5 μM curcumin increased TUNEL-positive cells after 24-h treatment, indicating that more cells displayed DNA fragmentation (Figure 7A). Our study focused on whether curcumin stimulates ROS production and $\Delta\Psi\text{m}$ levels. We demonstrated that ROS production was markedly elevated after the cells were treated with 12.5 μM curcumin at 12-h treatment (Figure 7B). To confirm whether the mitochondrial microenvironment included curcumin-induced cell apoptosis, the level of $\Delta\Psi\text{m}$ was measured. A375.S2/VR cells exhibited a decrease in $\Delta\Psi\text{m}$ after 12 h of curcumin treatment (Figure 7C).

3.7 | Effects of curcumin on caspase-9 and caspase-3 activities in A375.S2/VR cells

To investigate whether the apoptosis induced by curcumin was mediated through caspase activation, caspase-9 and caspase-3 activities were detected after curcumin exposure for 6, 12, and 24 h. Treatment with curcumin significantly and time-dependently stimulated the

FIGURE 2 Effects of curcumin on the viability of A375.S2 parental and A375.S2/VR cells. Both of the cells were individually treated with curcumin (6.25, 12.5, 25, and 50 μM) for 24 h. Cell viability of (A) A375.S2 parental cells, and (B) A375.S2/VR cells was determined via an MTT assay. Each point represents the mean \pm SD of three experiments; *** $p < .001$ versus control



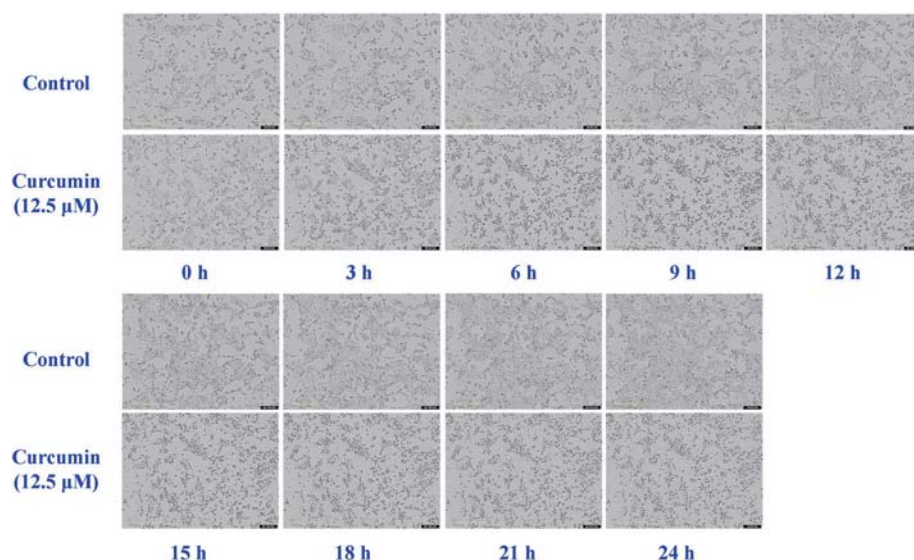


FIGURE 3 Effects of curcumin on the confluence of A375.S2/VR cells. The cells were seeded and treated with 12.5 μM curcumin for 24 h. Cell images were recorded and photographed at 0, 3, 6, 9, 12, 15, 18, 21, and 24 h. A cell confluence assay of A375.S2/VR cells was performed using an IncuCyte S3 ZOOM System instrument

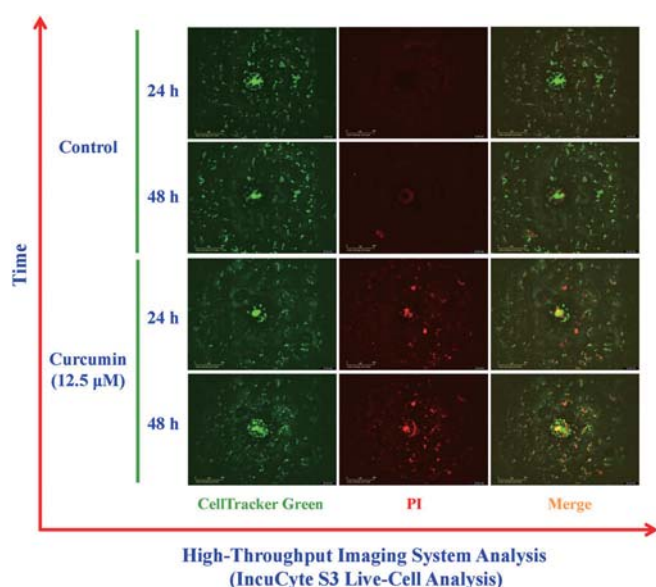


FIGURE 4 Effects of curcumin on A375.S2/VR cells in a 3D-spheroid cell death assay. The cells were seeded for 3 d before incubation with 12.5 μM curcumin for 24 h and 48 h. A375.S2/VR cells were stained with CellTracker Green (10 μM) before treatment with propidium iodide (PI) (1 $\mu\text{g}/\text{ml}$) to detect cell death using an IncuCyte S3 ZOOM System instrument

activities of both caspase-9 and caspase-3 (Figure 8A and B, respectively). In addition, specific caspase inhibitors (Z-VAD-FMK, Z-DEVD-FMK, and Z-LEHD-FMK) were applied to confirm caspase-9/caspase-3-mediated apoptosis by curcumin. Our results demonstrated that these 3 caspase inhibitors can significantly abolish curcumin-reduced cell viability by up to about 75%–80% (Figure 8C). Our data demonstrated that curcumin induced apoptosis, and the activation of caspase-9 and caspase-3 were involved in apoptotic cell death in A375.S2/VR cells.

3.8 | Curcumin-induced apoptosis is mediated by EGFR signaling pathway in A375.S2/VR cells

Many signaling cascades have been reported to be involved in curcumin-induced apoptosis.^{34–36} The mechanisms of drug resistance include alterations of the tumor microenvironment and reactivation of the EGFR, PI3K (phosphoinositide 3-kinase)/protein kinase B (AKT), and mitogen-activated protein kinase (MAPK) pathways.^{37–39} Our results showed that curcumin decreased the protein phosphorylation levels of EGFR, AKT, and ERK, without affecting its protein level (Figure 9A,B). Furthermore, gefitinib is an EGFR targeting inhibitor.⁴⁰ We further explored the anti-melanoma effects of curcumin combined with gefitinib on A375.S2/VR cells. The cells were cultured with 12.5 μM curcumin plus 20 μM gefitinib for 24 h. Our result demonstrated that combination treatment (curcumin plus gefitinib) synergistically potentiated the inhibitory effect on cell viability (Figure 9C). These data suggest a role for the EGFR signaling pathway in curcumin-induced apoptosis in A375.S2/VR cells.

4 | DISCUSSION

Curcumin is a natural compound that has been reported to inhibit several types of cancers, including pancreatic, prostate, breast, colorectal, leukemia, multiple myeloma, lung cancers, and melanoma.^{10,11} Because of the poor prognosis of patients with advanced melanoma, melanoma easily develops chemotherapy and targeted therapy resistance.⁴¹ There is an unmet need to find an effective therapy for these patients. To the best of our knowledge, this is the first study to report that curcumin effectively inhibited vemurafenib-resistant melanoma cells.

Curcumin has been reported to inhibit cancer cell growth via diverse signaling pathways, including apoptosis, cell cycle arrest, and autophagy.^{14,39,42,43} Liao *et al.* reported that curcumin induced apoptosis in human melanoma A375 cells through the reactive oxygen

FIGURE 5 Effects of curcumin on A375.S2/VR cell apoptosis. The cells were exposed to 12.5 μ M curcumin for 1, 2, 3, 4, 5, 6, 9, and 12 h. A375.S2/VR cells were then stained with Annexin V-FITC/PI before treatment with 4',6-diamidino-2-phenylindole (DAPI) (1 μ g/ml) to detect apoptosis in A375.S2/VR cells using Molecular Devices ImageXpress Micro Confocal

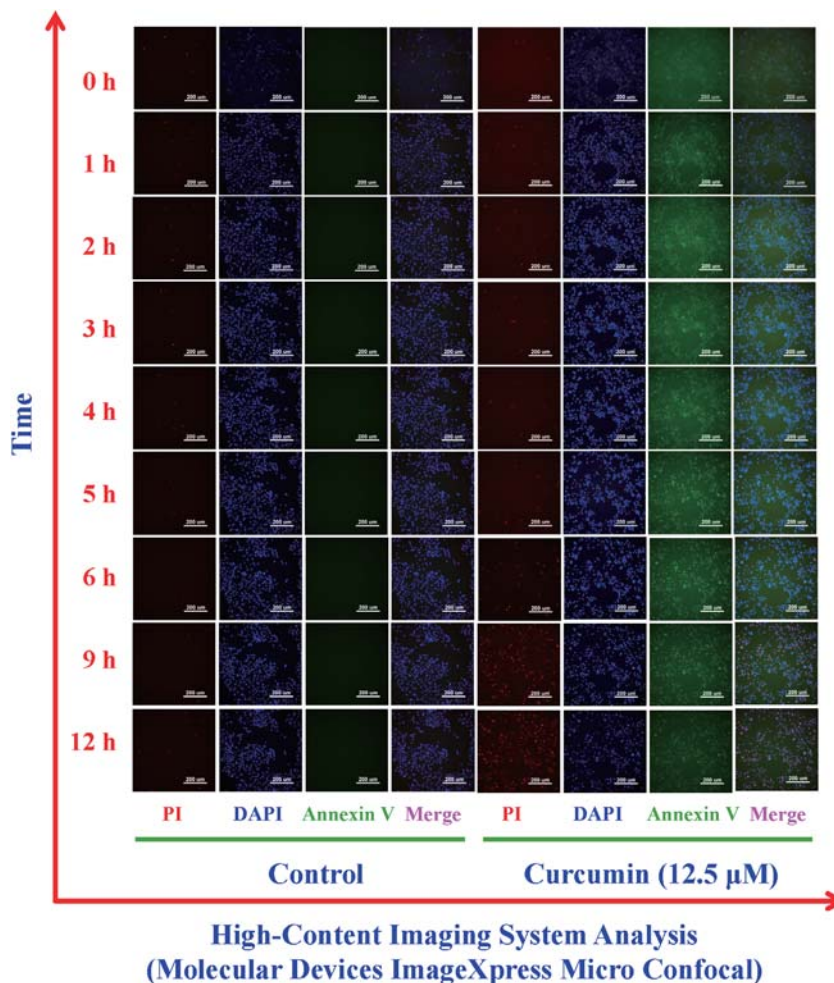
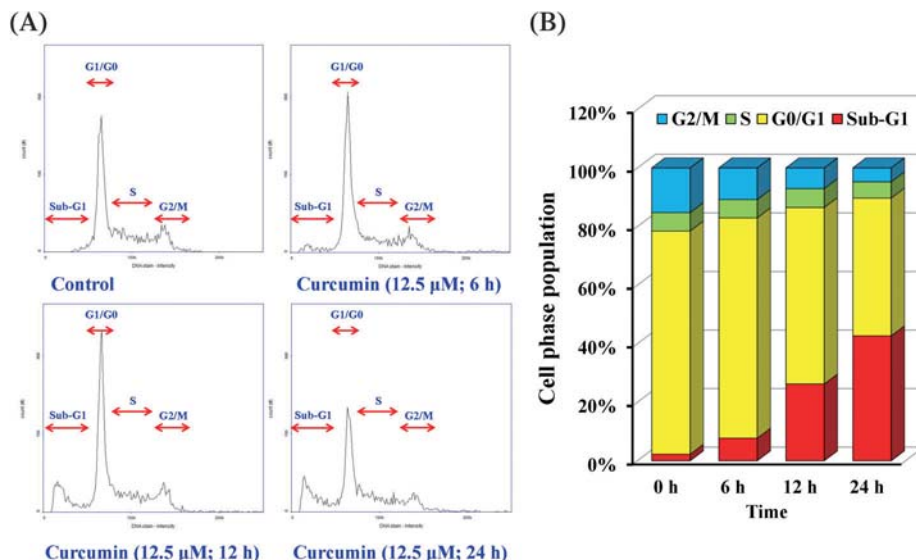


FIGURE 6 Effects of curcumin on A375.S2/VR cell cycle analysis. The cells were treated with 12.5 μ M curcumin for 6, 12, and 24 h. Cells were stained and determined. (A) Representative images of the cell cycle distribution, as determined using NucleoCounter NC-3000 imaging cytometry. (B) Quantification of G0/G1, S, G2/M phase, and sub-G1 population of % of cell phase population. Each experiment was performed in triplicate



species-dependent hypoxia-inducible factor-1 α (HIF-1 α) signaling pathway.¹³ Curcumin was found to inhibit A375 cell growth by inducing apoptosis and arresting the cell cycle.^{12,13,15-17} Moreover, curcumin can release cytochrome c from the mitochondria to the cytosol,

which is induced by mitochondria membrane potential disruption; curcumin-induced inhibition of cell proliferation and cell cycle arrest can be reversed by *N*-acetyl-l-cysteine.¹³ The results of the present study showed that curcumin induced A375.S2/VR cell apoptosis

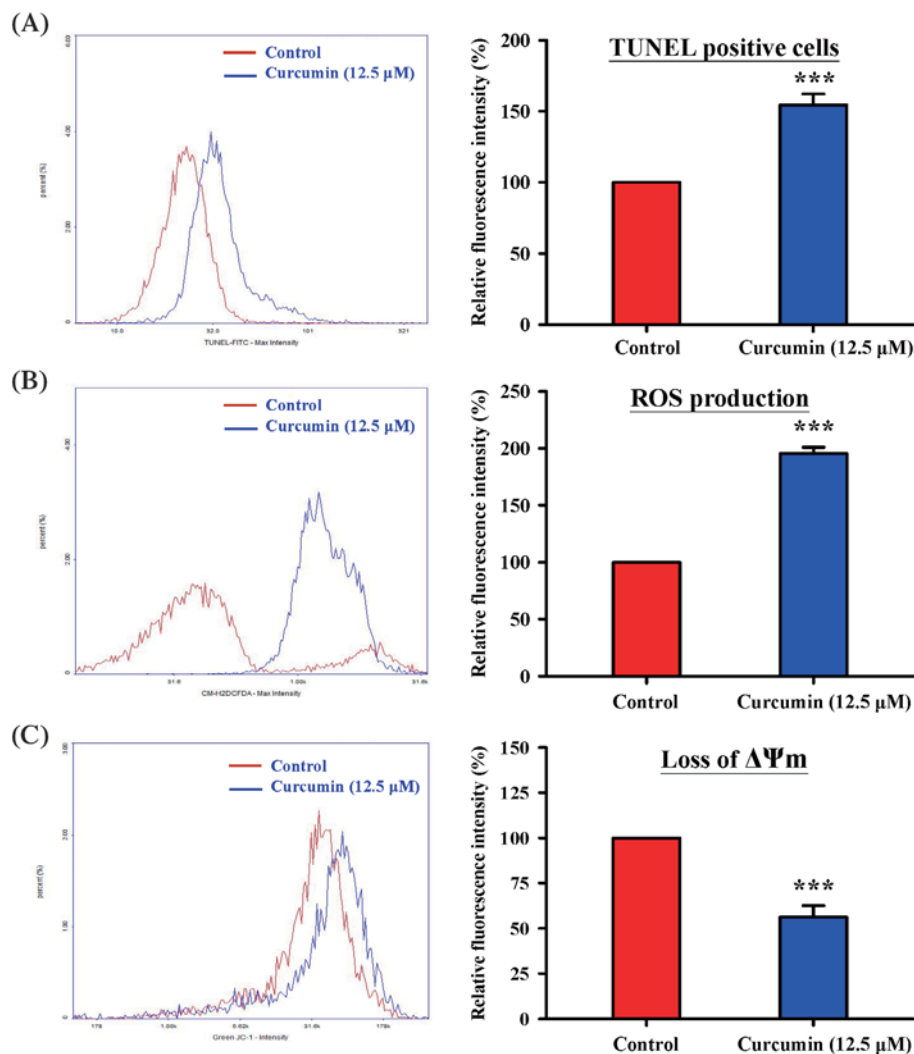


FIGURE 7 Effects of curcumin on A375.S2/VR cells in terminal deoxynucleotidyl transferase dUTP nick end labeling (TUNEL) staining, reactive oxygen species (ROS) production, and loss of mitochondrial membrane potential ($\Delta\Psi_m$). The cells were incubated with 12.5 μM curcumin for indicated periods of time. Representative profile of TUNEL-FITC fluorescence intensity (A, Left) was prepared. The cells were incubated with CM-H₂DCFDA and JC-1 by imaging cytometry. Representative profile of fluorescence intensity of ROS production (B, Left) and loss of $\Delta\Psi_m$ (C, Left) were performed. All quantitative data were shown (Right 3 panels). Each point represents the mean \pm SD of three experiments; *** $p < .001$ versus control. ### $p < .001$ versus curcumin only treatment

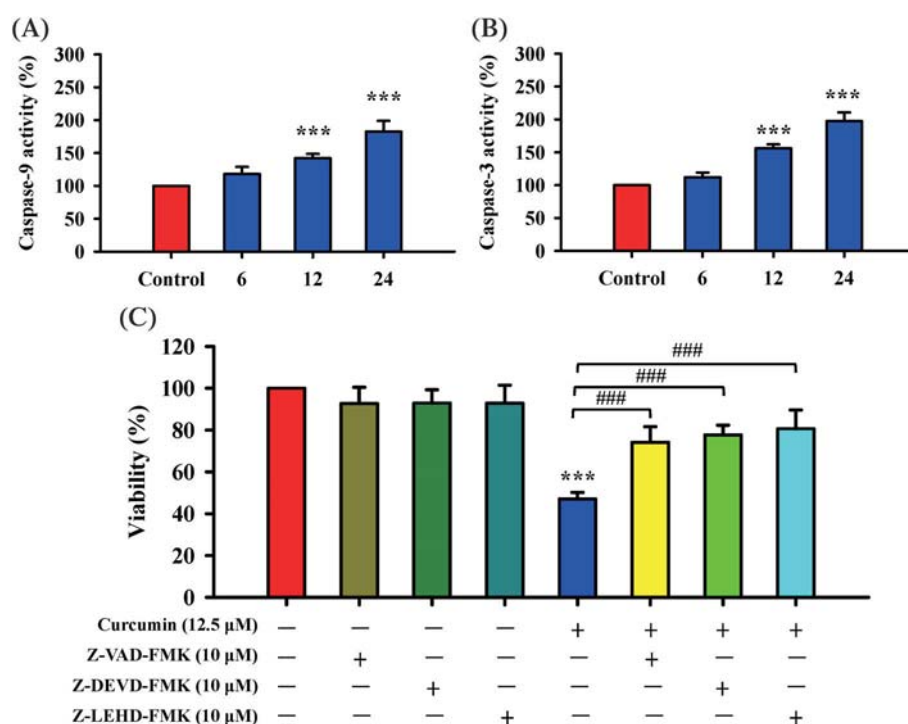


FIGURE 8 Effects of curcumin on caspase-9 and caspase-3 activities as well as viability after preincubation with specific caspases inhibitors in A375.S2/VR cells. The cells were exposed to 12.5 μM curcumin for 6, 12, and 24 h in the presence or absence of 10 μM Z-VAD-FMK (a pan-caspase inhibitor), 10 μM Z-DEVD-FMK (a caspase-3 inhibitor), or 10 μM Z-LEHD-FMK (a caspase-9 inhibitor) for 1 h pretreatment. The fluorochrome-labeled inhibitor of caspases assay (FLICA) method was applied using the FAM-FLICA Assay Kits, and the stained cells were detected via imaging cytometry. Quantitative analysis of the (A) caspase-9 and (B) caspase-3 activities was performed. (C) After treatment, cell viability was estimated using the MTT assay. Each point represents the mean \pm SD of three experiments; *** $p < .001$ versus control

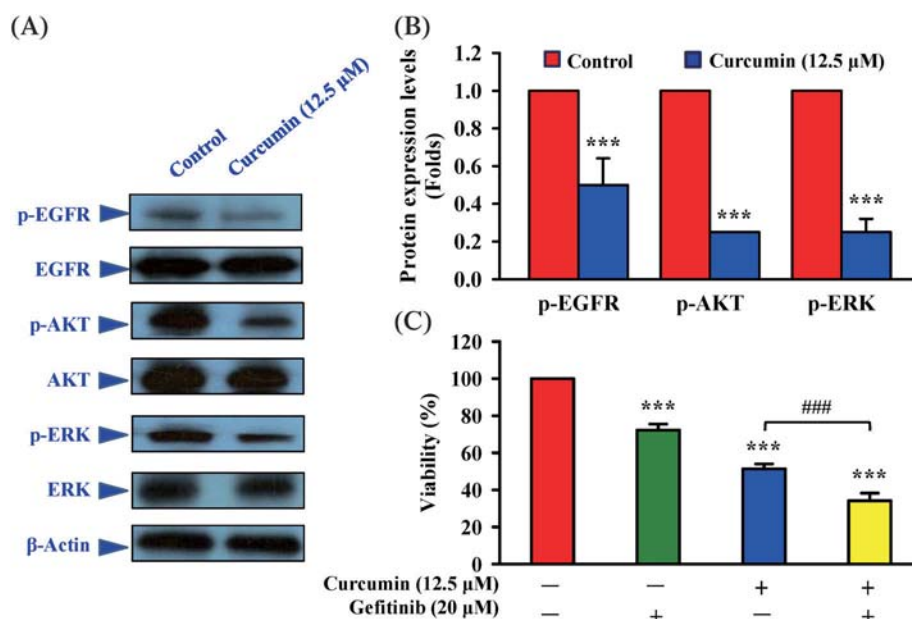


FIGURE 9 Effects of curcumin on EGFR, AKT, and ERK signaling in A375.S2/VR cells. The cells were seeded and treated with 12.5 μ M curcumin for 12 h. The cells were harvested, and a whole cell lysate was prepared and lysed. (A) The protein levels of p-EGFR, EGFR, p-AKT, AKT, p-ERK, and ERK were determined using western blotting analysis. All blots were normalized to β -actin to ensure the same loading. (B) Quantitative data of the blots are shown via NIH ImageJ program, and each point represents the mean \pm SD of two separate experiments. (C) The cells were cultured with 12.5 μ M curcumin combined with 20 μ M gefitinib (an EGFR inhibitor) for 24 h. The synergistic effect of viability was determined via the MTT assay, and each point represents the mean \pm SD of three separate experiments; *** p < .001 versus control. ### p < .001 versus curcumin only treatment

(Figures 5, 6, and 7A), ROS production (Figure 7B), and mitochondrial downstream signaling pathway (Figure 7C). Caspase-3 and -9 were increased in a time-dependent manner caused by curcumin (Figure 8).

Patients with advanced melanoma generally have a poor prognosis.²¹ Active mutated BRAF kinase has been reported to occur in more than 40% of patients with melanoma.⁴⁴ In recent years, the overall survival has been improved by both inhibitors of BRAF and MEK, such as vemurafenib, dabrafenib, trametinib, cobimetinib, and binimetinib.⁸ However, drug resistance generally developed in 1 year, which is the main obstacle for successful treatment.⁴⁵ The mechanisms of drug resistance include alterations of the tumor microenvironment and reactivation of the EGFR, PI3K (phosphoinositide 3-kinase)/protein kinase B (AKT) pathway, and the MAPK pathway.^{37–39,42} BRAF^{V600E} mutation is intrinsically resistant to BRAF inhibitors due to feedback activation of the EGFR in colorectal cancer.^{46,47} Combination with a BRAF inhibitor and an EGFR inhibitor can block reactivation of MAPK signaling in BRAF-mutant colorectal cancer cells, leading to significantly improve therapeutic efficacy.⁴⁷ The clinical evidence suggests that the mRNA levels of EGFR were improved in BRAF^{V600E} melanoma patients and strongly induced EGFR protein post-resistance. Additionally, the increased EGFR protein and mRNA levels express in vemurafenib-resistant A375 melanoma cells. Two major downstream signaling pathways (RAS/MEK/ERK and PI3K/AKT) contribute to EGFR signaling.⁴⁸ Su *et al.* generated and characterized a melanoma cell line that was resistant to vemurafenib treatment, suggesting that

reactivation of the RAS/RAF/MAPK and AKT pathway by upstream signaling activation may be a critical mechanism for melanoma acquiring resistance to vemurafenib.⁴⁹ Mogni *et al.* subsequently reported that the pan-RAF inhibitor sorafenib effectively synergizes with vemurafenib to block resistant cells.⁵⁰ Dratkiewicz *et al.* reported the increased levels of EGFR, MET, and selected markers of cancer stem cells in vemurafenib-resistant melanoma cell lines.⁵¹ Treatment with pairs of inhibitors against EGFR and MET induced a synergistic cytotoxic effect and inhibited invasiveness. EGFR, downstream signaling RAS/BRAF/MAPK, and PI3K/AKT could regulate resistance to the BRAF inhibitor (vemurafenib).⁵¹ Novel therapies need to be developed to combat resistance to BRAF inhibitors.

Curcumin has been thought to be one of the most encouraging natural compounds to exhibit anti-EGFR activity.⁵² Starok *et al.* reported that curcumin inhibits the receptor of kinase autophosphorylation by not only directly but also partially inhibiting the EGFR intracellular domain, but also affects the cell membrane environment of EGFR.⁵² Oliveira *et al.* reported that curcumin analogue DM-1 has substantial anti-proliferation activity in SKMEL-19, SKMEL-28, SKMEL-29, and A375 melanoma cells. DM-1 also showed growth inhibitory potential for four types vemurafenib-resistant melanoma cell lines (SKMEL-19R, SKMEL-28R, SKMEL-29R, and A375R).⁵³ Moreover, DM-1 significantly reduced the colony formation and cell migration by matrix metalloproteinase-1 (MMP-1), MMP-2 and MMP-9 inhibition, endothelial cell formation, and cell

cycle arrest in BRAF-resistant melanomas.⁵⁴ However, there are no reports regarding the correlation between curcumin and EGFR in melanoma cells. In the present study, the results of western blotting revealed that the EGFR and AKT/ERK kinase signaling pathway was downregulated after treatment with curcumin in A375.S2/VR cells (Figure 9). The preclinical study demonstrated that curcumin reduces the incidence of BRAF mutant colorectal cancer.⁵⁵ Qin *et al.* showed that curcumin analogs based oximes exhibited strong anti-melanoma activity by inhibiting BRAF^{V600E} and EGFR kinase activities *via in vitro* kinase activity assay.⁵⁶ However, there is no evidence regarding the effects of curcumin on cell models and animal experiments in A375.S2/VR cells and the involvement of cell growth in BRAF^{V600E} kinase activity. Importantly, our results showed that gefitinib and curcumin synergistically reduced cell viability in A375.S2/VR cells (Figure 9C). The application of combination therapy (an EGFR inhibitor and curcumin) may be a promising therapeutic candidate in BRAF-resistant melanomas.

5 | CONCLUSIONS

Our results revealed that curcumin suppresses tumor proliferation and induces apoptosis by arresting the cell cycle cascade, producing ROS, and decreasing mitochondrial membrane potential ($\Delta\Psi_m$); furthermore, EGFR signaling pathway was downregulated by curcumin in vemurafenib-resistant A375.S2 cells (A375.S2/VR cells). The present study sheds new light on the therapy of vemurafenib-resistant melanoma that curcumin may be an encouraging therapeutic candidate.

ACKNOWLEDGMENTS

The authors would like to thank Mr. Chang-Wei Li (AllBio Science Incorporated), Mr. Kai-Hsiang Chang, Mr. Chin-Chen Lin (Tekon Scientific Corp.), and Mr. Cheng-Wu Shih (Cell-Bio Biotechnology Co., Ltd.) for providing assistance and equipment. We also thank the Office of Research and Development, China Medical University (Taiwan) for providing Medical Research Core Facilities to perform the experiments and data analysis.

CONFLICT OF INTEREST

The authors declare that they have no conflicts of interest.

AUTHOR CONTRIBUTIONS

Yu-Jen Chiu, Jai-Sing Yang, and Jo-Hua Chiang: Conceived and designed the studies. Hong-Yi Chiu, Yu-Ning Juan, and Yu-Hsiang Lo: Performed the experiments. Yu-Jen Chiu, Jai-Sing Yang, Fuu-Jen Tsai, and Jo-Hua Chiang: Discussed the studies. Yu-Jen Chiu, Jai-Sing Yang, Yu-Ning Juan, Yu-Hsiang Lo, and Jo-Hua Chiang: Performed the data statistical analysis. Yu-Jen Chiu, Jai-Sing Yang, Fuu-Jen Tsai, and Jo-Hua Chiang: Prepared the final figures. Yu-Jen Chiu, Jai-Sing Yang, and Jo-Hua Chiang: wrote the paper. All authors read and approved the final manuscript.

ORCID

Jai-Sing Yang  <https://orcid.org/0000-0001-7302-8248>

Jo-Hua Chiang  <https://orcid.org/0000-0002-9316-1932>

REFERENCES

1. Welch HG, Mazer BL, Adamson AS. The rapid rise in cutaneous melanoma diagnoses. *N Engl J Med.* 2021;384(1):72-79.
2. Wongvibulsin S, Pahalyants V, Kalinich M, et al. Epidemiology and risk factors for the development of cutaneous toxicities in patients treated with immune-checkpoint inhibitors: a United States population-level analysis. *J Am Acad Dermatol.* 2021. doi:10.1016/j.jaad.2021.03.094. Online ahead of print.
3. McMeniman EK, Duffy DL, Jagirdar K, et al. The interplay of sun damage and genetic risk in Australian multiple and single primary melanoma cases and controls. *Br J Dermatol.* 2020;183(2):357-366.
4. Nahm SH, Rembielak A, Peach H, Lorigan PC, Contributing C. Consensus guidelines for the Management of Melanoma during the COVID-19 pandemic: surgery, systemic anti-cancer therapy, radiotherapy and follow-up. *Clin Oncol (R Coll Radiol).* 2021;33(1):e54-e57.
5. Hanson J, Demer A, Liszewski W, Foman N, Maher I. Improved overall survival of melanoma of the head and neck treated with Mohs micrographic surgery versus wide local excision. *J Am Acad Dermatol.* 2020; 82(1):149-155.
6. Molina G, Kasumova GG, Qadan M, Boland GM. Use of immunotherapy and surgery for stage IV melanoma. *Cancer.* 2020;126(11):2614-2624.
7. Blankenstern SA, Aarts MJ, Van Den Berkortel FW, et al. Surgery for unresectable stage IIIC and IV melanoma in the era of new systemic therapy. *Cancer.* 2020;12(5):1176.
8. Hima P, Yacoub N, Mishra R, et al. Current advances in the treatment of BRAF-mutant melanoma. *Cancer.* 2020;12(2):482.
9. Fujisawa Y, Ito T, Kato H, et al. Outcome of combination therapy using BRAF and MEK inhibitors among Asian patients with advanced melanoma: an analysis of 112 cases. *Eur J Cancer.* 2021;145:210-220.
10. Mazumder K, Biswas B, Raja IM, Fukase K. A review of cytotoxic plants of the Indian subcontinent and a broad-spectrum analysis of their bioactive compounds. *Molecules.* 2020;25(8):1904.
11. Stohs SJ, Chen O, Ray SD, Ji J, Bucci LR, Preuss HG. Highly bioavailable forms of curcumin and promising avenues for curcumin-based research and application: a review. *Molecules.* 2020;25(6):1397.
12. Szlasa W, Supplitt S, Drag-Zalesinska M, et al. Effects of curcumin based PDT on the viability and the organization of actin in melanotic (A375) and amelanotic melanoma (C32) - *in vitro* studies. *Biomed Pharmacother.* 2020;132:110883.
13. Liao W, Xiang W, Wang FF, Wang R, Ding Y. Curcumin inhibited growth of human melanoma A375 cells via inciting oxidative stress. *Biomed Pharmacother.* 2017;95:1177-1186.
14. Liczbinski P, Michalowicz J, Bukowska B. Molecular mechanism of curcumin action in signaling pathways: review of the latest research. *Phytother Res.* 2020;34(8):1992-2005.
15. Zhao G, Han X, Zheng S, et al. Curcumin induces autophagy, inhibits proliferation and invasion by downregulating AKT/mTOR signaling pathway in human melanoma cells. *Oncol Rep.* 2016;35(2):1065-1074.
16. Chen J, Li L, Su J, Li B, Chen T, Wong YS. Synergistic apoptosis-inducing effects on A375 human melanoma cells of natural borneol and curcumin. *PLoS One.* 2014;9(6):e101277.
17. Bill MA, Bakan C, Benson DM Jr, Fuchs J, Young G, Lesinski GB. Curcumin induces proapoptotic effects against human melanoma cells and modulates the cellular response to immunotherapeutic cytokines. *Mol Cancer Ther.* 2009;8(9):2726-2735.
18. Lo C, Lai TY, Yang JS, et al. Gallic acid inhibits the migration and invasion of A375.S2 human melanoma cells through the inhibition of

- matrix metalloproteinase-2 and Ras. *Melanoma Res.* 2011;21(4):267-273.
19. Acquaviva J, Smith DL, Jimenez JP, et al. Overcoming acquired BRAF inhibitor resistance in melanoma via targeted inhibition of Hsp90 with ganetespib. *Mol Cancer Ther.* 2014;13(2):353-363.
 20. Chueh FS, Chen YL, Hsu SC, et al. Triptolide induced DNA damage in A375.S2 human malignant melanoma cells is mediated via reduction of DNA repair genes. *Oncol Rep.* 2013;29(2):613-618.
 21. Hsiao YP, Yu CS, Yu CC, et al. Triggering apoptotic death of human malignant melanoma a375.s2 cells by bufalin: involvement of caspase cascade-dependent and independent mitochondrial signaling pathways. *Evid Based Complement Alternat Med.* 2012;2012:591241.
 22. Huang SH, Hsu MH, Hsu SC, et al. Phenethyl isothiocyanate triggers apoptosis in human malignant melanoma A375.S2 cells through reactive oxygen species and the mitochondria-dependent pathways. *Hum Exp Toxicol.* 2014;33(3):270-283.
 23. Lee MR, Lin C, Lu CC, et al. YC-1 induces G0/G1 phase arrest and mitochondria-dependent apoptosis in cisplatin-resistant human oral cancer CAR cells. *Biomedicine (Taipei).* 2017;7(2):12.
 24. Demuyneck R, Efimova I, Lin A, Declercq H, Krysko DV. A 3D cell death assay to quantitatively determine ferroptosis in spheroids. *Cell.* 2020;9(3):703.
 25. Lai GJ, Shalumon KT, Chen SH, Chen JP. Composite chitosan/silk fibroin nanofibers for modulation of osteogenic differentiation and proliferation of human mesenchymal stem cells. *Carbohydr Polym.* 2014;111:288-297.
 26. Saftescu S, Popovici D, Oprean C, et al. Determining factors of renal dysfunction during cisplatin chemotherapy. *Exp Ther Med.* 2021;21(1):83.
 27. Ha HA, Chiang JH, Tsai FJ, et al. Novel quinazolinone MJ33 induces AKT/mTOR-mediated autophagy-associated apoptosis in 5FU-resistant colorectal cancer cells. *Oncol Rep.* 2021;45(2):680-692.
 28. Liu SP, Shibu MA, Tsai FJ, et al. Tetramethylpyrazine reverses high-glucose induced hypoxic effects by negatively regulating HIF-1 α induced BNIP3 expression to ameliorate H9c2 cardiomyoblast apoptosis. *Nutr Metab (Lond).* 2020;17:12.
 29. Wu KM, Hsu YM, Ying MC, et al. High-density lipoprotein ameliorates palmitic acid-induced lipotoxicity and oxidative dysfunction in H9c2 cardiomyoblast cells via ROS suppression. *Nutr Metab (Lond).* 2019;16:36.
 30. Chiang JH, Tsai FJ, Hsu YM, Yin MC, Chiu HY, Yang JS. Sensitivity of allyl isothiocyanate to induce apoptosis via ER stress and the mitochondrial pathway upon ROS production in colorectal adenocarcinoma cells. *Oncol Rep.* 2020;44(4):1415-1424.
 31. Huang TY, Peng SF, Huang YP, et al. Combinational treatment of all-trans retinoic acid (ATRA) and bisdemethoxycurcumin (BDMC)-induced apoptosis in liver cancer Hep3B cells. *J Food Biochem.* 2020;44(2):e13122.
 32. Lin CC, Chen KB, Tsai CH, et al. Casticin inhibits human prostate cancer DU 145 cell migration and invasion via Ras/Akt/NF-kappaB signaling pathways. *J Food Biochem.* 2019;43(7):e12902.
 33. Lee HP, Wang SW, Wu YC, et al. Glucocerebroside reduces endothelial progenitor cell-induced angiogenesis. *Food Agr Immunol.* 2019;30(1):1033-1045.
 34. Dai X, Zhang J, Guo G, et al. A mono-carbonyl analog of curcumin induces apoptosis in drug-resistant EGFR-mutant lung cancer through the generation of oxidative stress and mitochondrial dysfunction. *Cancer Manag Res.* 2018;10:3069-3082.
 35. Zhan Y, Chen Y, Liu R, Zhang H, Zhang Y. Potentiation of paclitaxel activity by curcumin in human breast cancer cell by modulating apoptosis and inhibiting EGFR signaling. *Arch Pharm Res.* 2014;37(8):1086-1095.
 36. Sun XD, Liu XE, Huang DS. Curcumin induces apoptosis of triple-negative breast cancer cells by inhibition of EGFR expression. *Mol Med Rep.* 2012;6(6):1267-1270.
 37. Rujirachotiawat A, Suttamanatwong S. Curcumin promotes collagen type I, keratinocyte growth factor-1, and epidermal growth factor receptor expressions in the in vitro wound healing model of human gingival fibroblasts. *Eur J Dent.* 2021;15(1):63-70.
 38. Chiu YJ, Yang JS, Hsu HS, Tsai CH, Ma H. Adipose-derived stem cell conditioned medium attenuates cisplatin-triggered apoptosis in tongue squamous cell carcinoma. *Oncol Rep.* 2018;39(2):651-658.
 39. Ruiz de Porras V, Layos L, Martinez-Balibrea E. Curcumin: a therapeutic strategy for colorectal cancer? *Semin Cancer Biol.* 2021;73:321-330.
 40. Peng XR, Wang Q, Wang HR, Hu K, Xiong WY, Qiu MH. FPR2-based anti-inflammatory and anti-lipogenesis activities of novel meroterpenoid dimers from Ganoderma. *Bioorg Chem.* 2021;116:105338.
 41. Chu PY, Chen YF, Li CY, et al. Factors influencing locoregional recurrence and distant metastasis in Asian patients with cutaneous melanoma after surgery: a retrospective analysis in a tertiary hospital in Taiwan. *J Chin Med Assoc.* 2021;84(9):870-876.
 42. Chestnut C, Subramaniam D, Dandawate P, et al. Targeting major signaling pathways of bladder cancer with phytochemicals: a review. *Nutr Cancer.* 2021;73(11-12):2249-2271.
 43. Chiu YJ, Tsai FJ, Bau DT, et al. Nextgeneration sequencing analysis reveals that MTH3, a novel curcuminoid derivative, suppresses the invasion of MDAMB231 triplenegative breast adenocarcinoma cells. *Oncol Rep.* 2021;46(1):133.
 44. Ribas A, Daud A, Pavlick AC, et al. Extended 5-year follow-up results of a phase Ib study (BRIM7) of vemurafenib and cobimetinib in BRAF-mutant melanoma. *Clin Cancer Res.* 2020;26(1):46-53.
 45. Ziogas DC, Konstantinou F, Bouros S, Theochari M, Gogas H. Combining BRAF/MEK inhibitors with immunotherapy in the treatment of metastatic melanoma. *Am J Clin Dermatol.* 2021;22(3):301-314.
 46. Prahallad A, Sun C, Huang S, et al. Unresponsiveness of colon cancer to BRAF(V600E) inhibition through feedback activation of EGFR. *Nature.* 2012;483(7387):100-103.
 47. Corcoran RB, Ebi H, Turke AB, et al. EGFR-mediated re-activation of MAPK signaling contributes to insensitivity of BRAF mutant colorectal cancers to RAF inhibition with vemurafenib. *Cancer Discov.* 2012;2(3):227-235.
 48. Sun C, Wang L, Huang S, et al. Reversible and adaptive resistance to BRAF(V600E) inhibition in melanoma. *Nature.* 2014;508(7494):118-122.
 49. Su F, Bradley WD, Wang Q, et al. Resistance to selective BRAF inhibition can be mediated by modest upstream pathway activation. *Cancer Res.* 2012;72(4):969-978.
 50. Mologni L, Costanza M, Sharma GG, et al. Concomitant BCORL1 and BRAF mutations in vemurafenib-resistant melanoma cells. *Neoplasia.* 2018;20(5):467-477.
 51. Dratkiewicz E, Simiczyjew A, Pietraszek-Gremplewicz K, Mazurkiewicz J, Nowak D. Characterization of melanoma cell lines resistant to vemurafenib and evaluation of their responsiveness to EGFR- and MET-inhibitor treatment. *Int J Mol Sci.* 2019;21(1):113.
 52. Starok M, Preira P, Vayssade M, Haupt K, Salomé L, Rossi C. EGFR inhibition by curcumin in cancer cells: a dual mode of action. *Bio-macromolecules.* 2015;16(5):1634-1642.
 53. Oliveira EA, Lima DS, Cardozo LE, et al. Toxicogenomic and bioinformatics platforms to identify key molecular mechanisms of a curcumin-analogue DM-1 toxicity in melanoma cells. *Pharmacol Res.* 2017;125(Pt B):178-187.
 54. de Souza N, de Oliveira EA, Faiao-Flores F, et al. Metalloproteinases suppression driven by the curcumin analog DM-1 modulates invasion in BRAF-resistant melanomas. *Anticancer Agents Med Chem.* 2020;20(9):1038-1050.
 55. Kane AM, Liu C, Akhter DT, et al. Curcumin chemoprevention reduces the incidence of Braf mutant colorectal cancer in a preclinical study. *Dig Dis Sci.* 2021;66(12):4326-4332.

56. Qin HL, Leng J, Youssif BGM, et al. Synthesis and mechanistic studies of curcumin analog-based oximes as potential anticancer agents. *Chem Biol Drug Des.* 2017;90(3):443-449.

SUPPORTING INFORMATION

Additional supporting information may be found in the online version of the article at the publisher's website.

How to cite this article: Chiu Y-J, Yang J-S, Tsai F-J, et al. Curcumin suppresses cell proliferation and triggers apoptosis in vemurafenib-resistant melanoma cells by downregulating the EGFR signaling pathway. *Environmental Toxicology.* 2022; 1-12. doi:10.1002/tox.23450